ISBN: 978-3-95450-200-4 doi:10.18429/JACoW-PCaPAC2018-THCA3

A FEEDBACK/FEEDFORWARD SYSTEM AT THE TPS AND ITS COMPONENT PERFORMANCE

C. H. Huang†, P. C. Chiu, K. H. Hu, Y. S. Cheng, C. Y. Wu, K. T. Hsu
NSRRC, Hsinchu 30076, Taiwan

Abstract

For a low-emittance photon light source like the Taiwan Photon Source (TPS), beam stability is a very important property for high-quality photon beams. It is, however, hard to completely remove beam disturbing effects. Therefore, a feedback/feedforward system becomes an effective tool to suppress beam motion. In this report, we discuss the performance of such a system implemented at the TPS. The component performance of the feedback system has been tested to understand its bandwidth limitations.

INTRODUCTION

The Taiwan Photon Source (TPS) is a third-generation light source at the NSRRC with 24 double-bend achromatic cells and a beam emittance of 1.6 nm-rad [1]. To achieve a high-quality beam, the beam motion must be controlled to within 10 % of the beam size or less. The vertical beam size in the center of the straight sections is around 5 μm making it necessary to control the beam motion to better than 0.5 μm.

There are many sources which may adversely affect beam stability[2]. Much effort have been spent to remove or eliminate such perturbations [3]. However, it is hard to remove all kinds of adverse effects. Therefore, a feedback/feedforward system has been developed to counteract beam motions. At first, the components of the feedback/feedforward system are introduced in this paper. The performance and computation model are described in the second part. Third, the performance of the feedback components are discussed and the bandwidth limitations of the fast orbit feedback system is determined.

FAST ORBIT FEEDBACK SYSTEM

There are 24 cells in the storage ring of the TPS, each including seven beam position monitors (BPMs), seven slow correctors and four fast correctors in each cell [4] as shown in Fig 1. The kick angle for the fast horizontal/vertical corrector is 4.8/12 μrad/A, respectively. There are mainly two types of BPMs installed in the storage ring. The k_x/k_y of standard BPMs, which are installed in the arc sections are 13.8/12.73 mm whereas the k_x/k_y of the primary BPMs, installed in the straight sections, are 6.58/8.89 mm. The eight (4 horizontal + 4 vertical) fast corrector power supplies in each cell are controlled by one corrector power supply controller (CPSC).

Libera brilliance+ is used as the BPM electronics. Each BPM platform deals with signal processing of four BPMs resulting in two platforms per cell. The electronics includes custom-written applications with VirtexTM 5 and Virtex 6 to be used for orbit feedback computations. One platform is responsible for the four horizontal correctors per cell and the second platform for the four vertical correctors. The correction rate is 10 kHz and the platform infrastructure is shown in Fig. 2. The bandwidth of the FOFB, shown in Fig. 3, is around 300 Hz in both the horizontal and vertical plane [5].

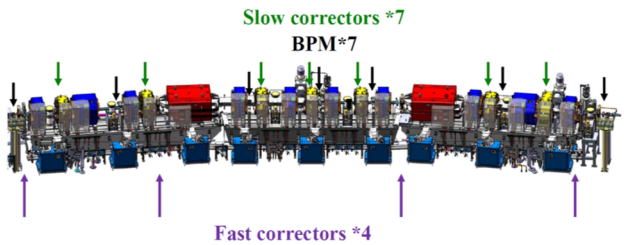

Figure 1: The location of beam position monitors (BPMs), slow and fast correctors in each cell.

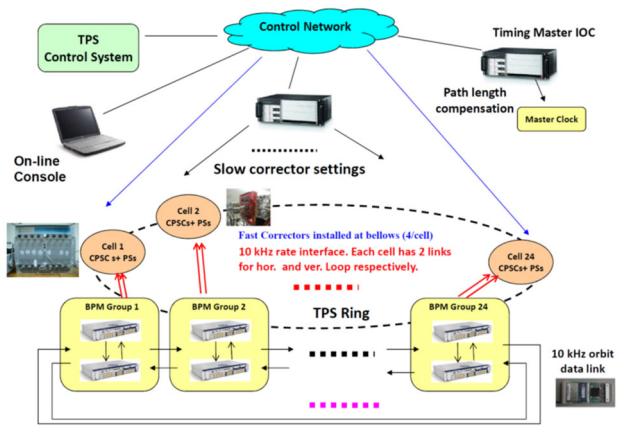

Figure 2: The infrastructure of the fast orbit feedback system.

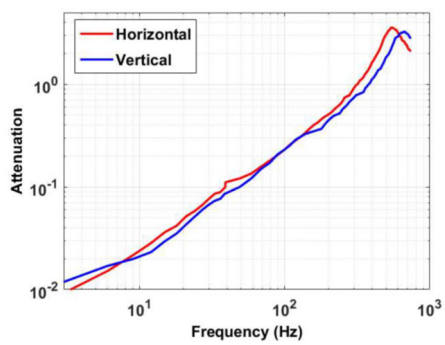

Figure 3: Frequency response of the fast orbit feedback system.

† huang.james@nsrrc.org.tw

ISBN: 978-3-95450-200-4 doi:10.18429/JACoW-PCaPAC2018-THCA3

RADIO FREQUENCY ADJUSTEMENT

As the FOFB is applied to correct beam motions or orbit drifts, we observe that the output current of the second and third fast corrector in each cell varies significantly compared to the other two due to the correction of path length changes. Although the FOFB system can compensate for path length changes during a short time period, the orbit drifts still increase by tens of microns per day of operation. Therefore, it is necessary to adjust the radio frequency to compensate for path length changes.

The radio frequency (RF) adjustment, as shown in Fig. 4, uses all fast horizontal corrector currents, $\Delta \boldsymbol{I}$, as obtained by the FOFB, and converts them to orbit drifts by the response matrix($\boldsymbol{R}$) at one Hz. With the dispersion matrix $\boldsymbol{D}$, the RF frequency change $\Delta \boldsymbol{F}$ [6] is given by

$$\Delta \boldsymbol{F} = \boldsymbol{D}^{-1}\boldsymbol{R}\Delta \boldsymbol{I}. \quad (1)$$

The RF frequency adjustments shows two peaks per day, as shown in Fig. 5, due to the earth tide. The radio frequency trends higher day by day due the decrease of ambient air temperature.

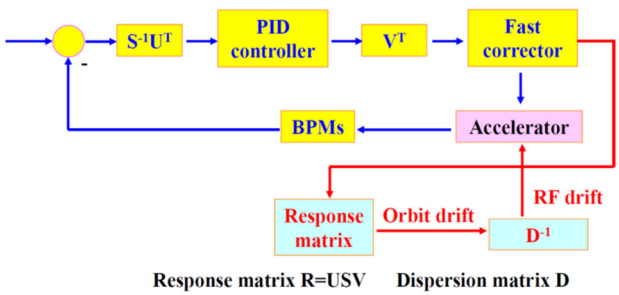

Figure 4: Scheme of the radio frequency (RF) adjustment.

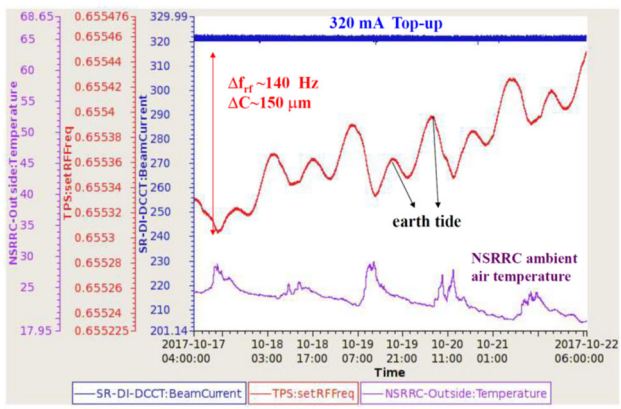

Figure 5: Radio frequency and ambient air temperature as a function of time.

PERFORMANCE OF THE COMPONENTS OF FEEDBACK SYSTEM

The 60 Hz beam motion in the vertical direction is more significant (~ 5 μm) than at other frequencies due to the RF transmitter and cooling fans for BPMs and nearby bellows [3], as shown in Fig. 6. In order to eliminate such 60 Hz beam motion, a feedforward correction is implemented because the 60 Hz perturbations are quite stable. At first, the beam motion, $\boldsymbol{b}(t)$, for all BPMs is recorded for one second simultaneously. The beam motion at 60 Hz in each BPM can be obtained by a Fourier transform of the beam position $\boldsymbol{B}(60) = \int_0^T \boldsymbol{b}(t)e^{-i2\pi*60*t}dt$ and the result is generally a complex number. Applying the inverse response matrix $\boldsymbol{R}^{-1}$ to the 60 Hz beam motion, $\boldsymbol{B}(60)$, we get the corrector strength to eliminate the 60 Hz beam motion from $\boldsymbol{C}(60) = -\boldsymbol{R}^{-1}\boldsymbol{B}(60)$. Because of unavoidable errors in the orbit and response matrix measurements singularities can appear resulting in unreasonably large and competing corrector strengths caused mostly by noise rather than error sources. We use therefore singular value decomposition (SVD) to rewrite the response matrix as $\boldsymbol{R} = \boldsymbol{USV}$ [7] and properly choose a singularity rejection parameter. The corrector strengths are then $\boldsymbol{C} = -\boldsymbol{V}^T\boldsymbol{S}^{inv}\boldsymbol{U}^T\boldsymbol{B}$, where the corrector strength would be a complex number as well and written as $C_j exp(i\phi_j)$. Here C_j is the amplitude of the j^{th} power supply and ϕ_j is the related phase [8].

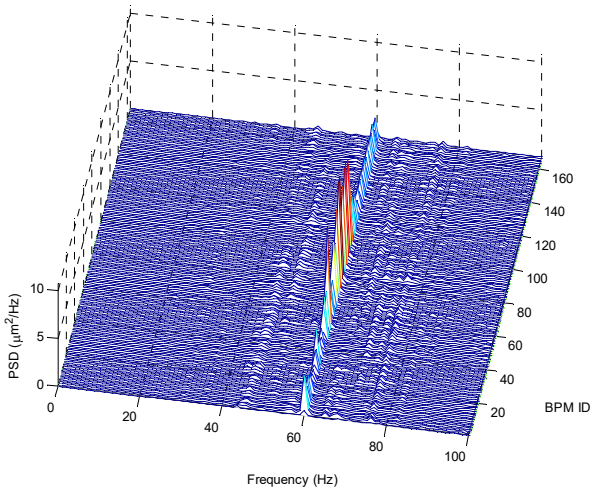

Figure 6: Power spectral density of the vertical beam motion.

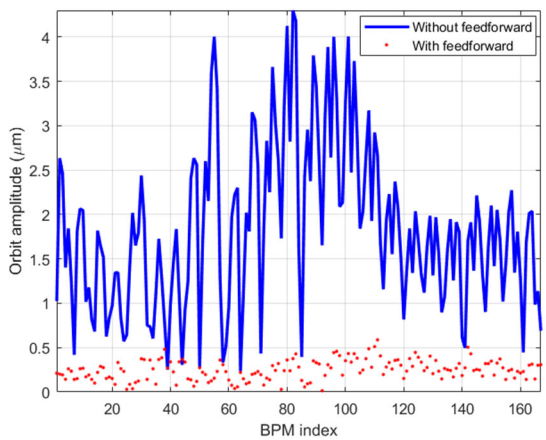

Figure 7: 60 Hz beam motion with and without feedforward correction.

With the correcting power supply generating a waveform, i.e. $C_j \cos(2\pi*60*t+\phi_j)$, the 60 Hz beam motion is corrected. Note, that the 60 Hz beam motion comes from the mains powering the electronics. The mains frequency is not exactly 60 Hz and changes depending on the total load. Therefore, the waveform should be locked to the

ISBN: 978-3-95450-200-4 doi:10.18429/JACoW-PCaPAC2018-THCA3

phase of the mains. Figure 7 shows that the 60 Hz beam motion is reduced to 1/10 with feedforward correction compared to no feedforward correction.

COMPONENT PERFORMANCE OF THE FOFB SYSTEM

In the second section we discussed that the bandwidth of the FOFB is roughly 300 Hz in both planes. In order to understand the limitation of this feedback system, the performance of each component, i.e. power supply, power supply controller, magnet, vacuum chamber and BPMs must be evaluated. A sweeping sine wave is generated by a waveform generator and sent into the controller of the power supply, as shown in Fig. 8, to measure the frequency response of the fast corrector and vacuum chamber. As the output current and the magnetic field is sent into the same analog-to-digital convertor (ADC), the magnetic field response and phase lag with respect to the output current of the power supply can be obtained.

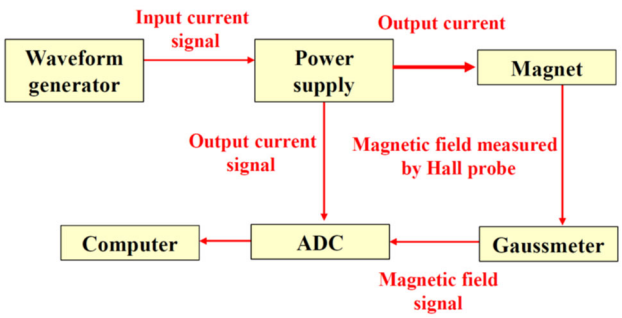

Figure 8: Block diagram for the measurement of dynamic magnetic field response.

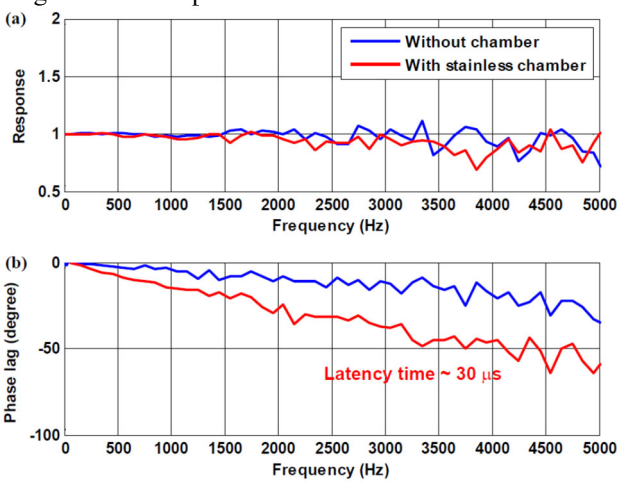

Figure 9: Frequency response (a) and field phase lag (b) of the fast correctors with and without vacuum chamber relative to the power supply output current.

From the frequency response of the fast correctors in Fig. 9, we find that the amplitude attenuation is quite low below 5 kHz. A phase lag can be observed and from $\phi=2\pi ft$, where ϕ, f and t are phase lag, frequency, and time lag, respectively, we estimate the latency time to be ~ 30 μsec for the magnetic field measured in the stainless vacuum chamber..

Homemade fast corrector power supplies [9] are used in in the FOFB. Proportional integral (PI) controls are used in these power supplies. As the K_p parameter is increased, the bandwidth of the power is higher and the phase lag decreases, as shown in Fig. 10. However, at high K_p-values, such as 1.5, a resonance can be observed above 5 kHz in a constant current output, which leaves an ample operational range to adjust the power supply for a high bandwidth, low phase lag and high stability.

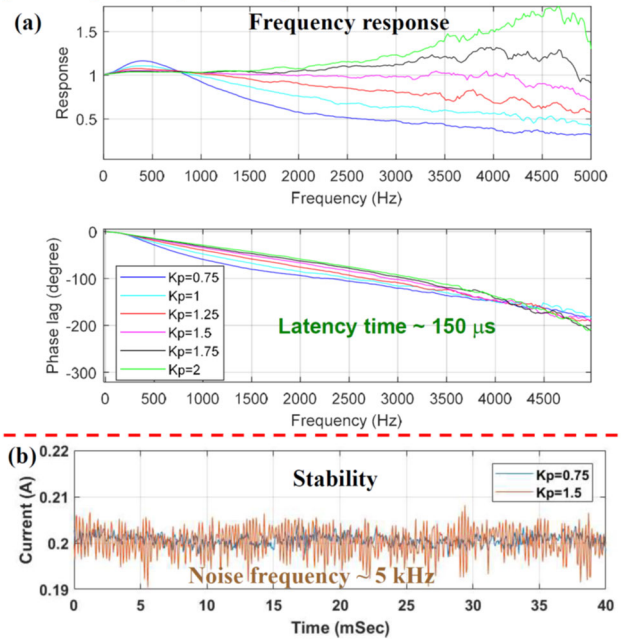

Figure 10: Performance (a) and stability (b) of the fast corrector power supplies for different K_p.

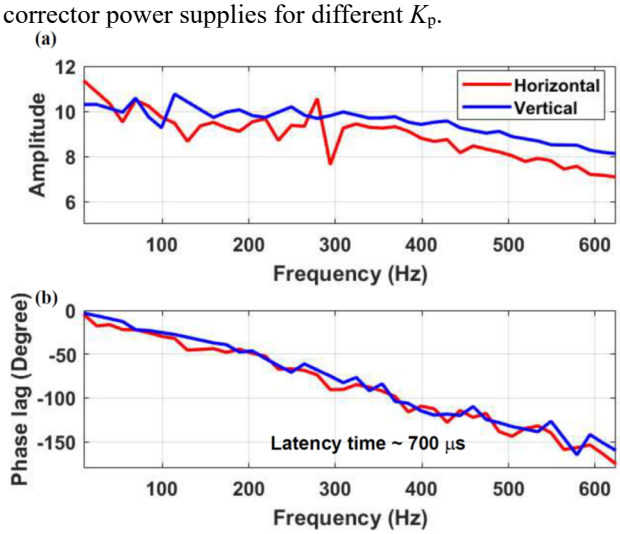

Figure 11: Frequency response and phase lag of the beam with respect to the current setting of the power supply.

The bandwidth and processing latency of the BPM electronics is approximately 2 kHz and 270 μsec and the latency of the CPSC is around 100 μsec. As to the overall contribution to the beam, we observe that the amplitude attenuation is low for frequncies from 0 Hz to 600 Hz. The phase lag, though, is quite large and approximately 150° at 600 Hz. Therefore, the reduction of the phase lag is important for a large bandwidth of the FOFB.

ISBN: 978-3-95450-200-4 doi:10.18429/JACoW-PCaPAC2018-THCA3

CONCLUSION

To eliminate beam motion, a fast orbit feedback (FOFB) was implemented after initial beam commissioning. The bandwidth is about 300 Hz in both planes. To minimize orbit distortions, caused by a path length change due to the earth tide or ambient air temperature, the radio frequency is adjusted as follows. Because a vertical 60 Hz beam motion is dominant after applying the FOFB, a feedforward correction was proposed and put in operation this year.

From the analysis of the FOFB system components, the amplitude attenuation of the magnetic field detected by the beam is negligible as the frequency of the alternating current given by the power supply is increased. However, the phase lag should be reduced to increase the bandwidth of the FOFB.

REFERENCES

[1] C.C. Kuo, *et al.,* "Commissioning of the Taiwan Photon Source", in *Proc. IPAC'15*, Richmond, VA. USA, May 2015, paper TUXC3, pp. 1314–1318.

[2] R.O. Hettel, "Beam stability at light sources", *Rev. Sci. Instrum*. 73 (2002) 1396-1401.

[3] C. H. Huang, *et al.,* "Study of 60 Hz beam orbit fluctuations in the Taiwan Photon Source", in *Proc. IPAC'*17, Copenhagen, Denmark, May 2017, paper TUPAB107, pp. 1566–1569.

[4] P. C. Chiu, *et al.,* "Fast orbit scheme and implementation for TPS", in *Proc. IPAC'*13, Shanghai, China, May 2013, paper TUOCB202, pp. 1146–1148.

[5] P. C. Chiu, *et al.,* "Preliminary beam test for TPS fast orbit feedback system", in *Proc. IPAC'*16, Busan, Korea, paper WEPOW04, pp. 2930–2932.

[6] P. C. Chiu, *et al.,* "Orbit correction with path length compensation based on RF frequency adjustments in TPS", in *Proc. IPAC'*17, Copenhagen, Denmark, May 2017, paper TUPAB103, pp. 1553–1555.

[7] Y. Chuang, *et al.,* "Closed orbit correction using singular value decomposition of the response matrix", in *Proc. PAC'93*, Washington, USA, May 1993, pp. 2263–2265.

[8] C. H. Huang, *et al*., "Methods to detect error sources and their application at the TPS", in *Proc. IPAC'*18, Copenhagen, Denmark, May2017, paper WEPAL057, pp. 2305–2308.

[9] K. B. Liu, "Rigorous mathematical modelling for a fast corrector power supply in TPS", Jinst. 12 (2017) T04004.